phys. stat. sol. (a) **202**, No. 8, R79–R81 (2005) / **DOI** 10.1002/pssa.200510026

pss +++rapid research letters+++
www.pss-rapid.com

Ag–$Ag_{0.08}V_2O_5 \cdot nH_2O$ composite films as host materials for Li^+ intercalation

Ying Wang[*, 1], **Kyoungho Lee**[1, 2], **Huamei Shang**[1], **Benjamin Wiley**[3], **Younan Xia**[3], **and Guozhong Cao**[1]

[1] Department of Materials Science and Engineering, University of Washington, Seattle, WA, USA
[2] Division of Materials and Chemical Engineering, Soonchunhyang University, Chungnam, Korea
[3] Department of Chemistry, University of Washington, Seattle, WA, USA

Received 5 April 2005, revised 25 April 2005, accepted 27 April 2005

PACS 61.10.Nz, 68.37.Hk, 82.45.Xy, 82.47.Aa

---

[*] Corresponding author: e-mail ywjane@u.washington.edu, Phone: +01 206 543 3130, Fax: +01 206 543 3100

We have prepared Ag–$Ag_{0.08}V_2O_5 \cdot nH_2O$ composite films by dispersing Ag nanowires into $V_2O_5 \cdot nH_2O$ sol and have investigated electrochemical properties of the films for Li^+-ion intercalation applications. With the molar ratio of Ag nanowires to $V_2O_5 \cdot nH_2O$ as 0.1, such prepared films are composed of metallic Ag nanowires embedded in the matrix of $Ag_{0.08}V_2O_5 \cdot nH_2O$, due to partial Ag reacted with $V_2O_5 \cdot nH_2O$. At a current density of 85 mA/g, such Ag–$Ag_{0.08}V_2O_5 \cdot nH_2O$ film can intercalate about two equivalents of Li ions and delivers twice the capacity of the $V_2O_5 \cdot nH_2O$ xerogel film. Such improved electrochemical performance is ascribed to the changes in the microstructure and crystallinity of the Ag–$Ag_{0.08}V_2O_5 \cdot nH_2O$ films including (i) further amorphization of $V_2O_5 \cdot nH_2O$, (ii) increased porosity, and (iii) enhancement of electrical conductivity.

1 Introduction Vanadium pentoxide (V_2O_5) has a layered structure and is a promising cathode material for lithium secondary batteries [1]. Amorphous or low-crystalline $V_2O_5 \cdot nH_2O$ has higher Li^+ intercalation capacity than its crystalline analogue, due to several advantages such as small particle size, low density, and most importantly, no phase transition limits [2]. However, $V_2O_5 \cdot nH_2O$ xerogel films share the same disadvantage of low conductivity with crystalline V_2O_5. This problem can be solved by two methods. One is to form composites of V_2O_5 with other conductive materials such as carbon or metal. Recently, we have demonstrated that the intercalation capacity and rate can be drastically improved when a thin layer of $V_2O_5 \cdot nH_2O$ was coated on Ni nanorod arrays [3]. The other approach is to prepare metal-doped vanadium pentoxide, such as $M_xV_2O_5$ (M = Cu, Ag, and Ni) by introducing metal ions between the layers of the V_2O_5 structure [4]. The present work combines these two methods by incorporating Ag nanowires into the $Ag_xV_2O_5 \cdot nH_2O$ matrix to prepare the Ag–$Ag_xV_2O_5 \cdot nH_2O$ composite film and investigates its electrochemical properties as host materials for Li-ion intercalation. The relationship between the intercalation properties, electrical conductivity, and crystallinity has been discussed.

2 Experimental The detailed synthetic process of silver nanowires can be found in the previous publications of Xia's group [5]. $V_2O_5 \cdot nH_2O$ sols were synthesized with V_2O_5 (Alfa Aesar) and 30% H_2O_2 (J. T. Baker) as precursor. 0.136 g of V_2O_5 powder was dissolved in 7 ml H_2O and 0.603 ml H_2O_2 solution, followed by sonication until a yellow-brown gel was obtained. The resultant gel was then redispersed in deionized H_2O in the concentration of 0.01 mol/l vanadium and a brown clear sol was obtained. The Ag–$Ag_xV_2O_5 \cdot nH_2O$ composite film was prepared by mixing a certain volume of Ag nanowire suspension with 65 µl $V_2O_5 \cdot nH_2O$ sol quickly then spreading onto ITO substrate. The sample was then dried under ambient condition. For comparison purposes, $V_2O_5 \cdot nH_2O$ film was also prepared by spreading 65 µl $V_2O_5 \cdot nH_2O$ sol on ITO substrate and dried under ambient condition. Scanning electron microscopes (SEM), X-ray diffraction (XRD) and the four-point probe were used to characterize the Ag–$Ag_xV_2O_5 \cdot nH_2O$ and $V_2O_5 \cdot nH_2O$ films. The total amount of Ag in the film was characterized by dissolving Ag nanowires entirely in 65 µl V_2O_5 sol until no metallic Ag peaks were found in XRD, followed by characterization with SEM-EDS to attain the ratio of Ag/V_2O_5. Because the binding energies of Ag(0) and Ag(+1) are close, the

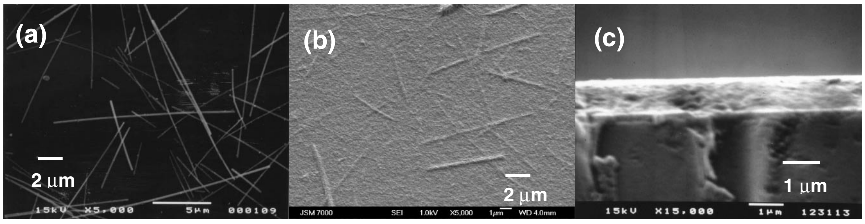

Figure 1 SEM images of (a) Ag nanowires, (b) top view of Ag–$Ag_{0.08}V_2O_5\cdot nH_2O$ film and (c) cross section of Ag–$Ag_{0.08}V_2O_5\cdot nH_2O$ film.

amount of Ag(0) and Ag(+1) in the composite film cannot be distinguished with X-ray photo-electron spectroscopy (XPS) [6]. Therefore, we measured XRD of a certain amount of silver and calculated the amount of metallic Ag in the Ag–$Ag_xV_2O_5\cdot nH_2O$ composite film by comparing the peak height of Ag(0) in such composite film to that of the known amount of Ag(0). For the composite film with molar ratio Ag/V_2O_5 = 0.1, the metallic Ag was found to be 20% of entire silver in the composite film, i.e., x was 0.08 in Ag–$Ag_xV_2O_5\cdot nH_2O$. Electrochemical properties of $V_2O_5\cdot nH_2O$ film and Ag–$Ag_{0.08}V_2O_5\cdot nH_2O$ film electrode were investigated using a standard three-electrode cell, with the 1M-$LiClO_4$ solution in propylene carbonate as the electrolyte, Pt mesh as the counter electrode and Ag/$AgNO_3$ as the reference electrode.

3 Results and discussion Figure 1a shows the SEM micrograph of silver nanowires dried on the glass substrate. The Ag nanowires have a diameter of ~300 nm and a length up to several tens of microns. These Ag nanowires are smooth, uniform, and mono-dispersed, which ensures their well-separated dispersion into $V_2O_5\cdot nH_2O$. Figure 1b shows the SEM micrograph of Ag–$Ag_{0.08}V_2O_5\cdot nH_2O$ composite film (molar ratio Ag/$V_2O_5\cdot nH_2O$ = 0.1) deposited on ITO substrate (top view). It can be seen that Ag nanowires are embedded in the relatively fine and smooth film. Cross section of the same film is shown in Fig. 1c. XRD patterns of Ag–$Ag_{0.08}V_2O_5\cdot nH_2O$ and $V_2O_5\cdot nH_2O$ films are presented in Fig. 2. The XRD of $V_2O_5\cdot nH_2O$ xerogel film displays the (00*l*) peaks and is in good agreement with the literature [7]. The XRD pattern of Ag–$Ag_{0.08}V_2O_5\cdot nH_2O$ film bears Ag peak and confirms that metallic Ag nanowires are embedded in the film. However, it is known that Ag and V_2O_5 react even at room temperature [4]. In comparison with diffraction peaks of $V_2O_5\cdot nH_2O$ film, the position shift and reduction in intensity of (001) and (003) peaks of Ag–$Ag_{0.08}V_2O_5\cdot nH_2O$ film can only be associated with the reaction between Ag and $V_2O_5\cdot nH_2O$. A small amount of silver can be intercalated between the layers of $V_2O_5\cdot nH_2O$ and affect the interlayer distance, though the parental layered structure is preserved. The resultant product is doped vanadium pentoxide, i.e., $Ag_{0.08}V_2O_5\cdot nH_2O$. The shift of (001) peak in $Ag_{0.08}V_2O_5\cdot nH_2O$ to higher angles suggests a reduction of the basal distance. The $V_2O_5\cdot nH_2O$ has a (001) peak at 7.515°, corresponding to an interlayer spacing of 11.75 Å, which is similar to 11.5 Å reported in the literature [7]. The $Ag_{0.08}V_2O_5\cdot nH_2O$ has a (001) peak at 9.644°, corresponding to an interlayer spacing of 9.16 Å which is obviously smaller than the interlayer spacing of $V_2O_5\cdot nH_2O$. The water content n in our $Ag_{0.08}V_2O_5\cdot nH_2O$ and $V_2O_5\cdot nH_2O$ is 1.6 (TGA profile not shown here, but reported in our separate publication [8]). The flattening of (003) peak indicates more amorphization of the structure. Such occurrence has also been observed in V_2O_5 gels doped by Ag powder as reported in the literature, in which the interlayer spacing decreases with increasing doping amount of Ag [4]. This shrinkage of interlayer spacing is ascribed to Ag^+ ions exerting a shielding effect on the negative charges on the oxygen ions of the VO_5 pyramids. Such shielding effect reduces the electrostatic repulsion force between two adjacent

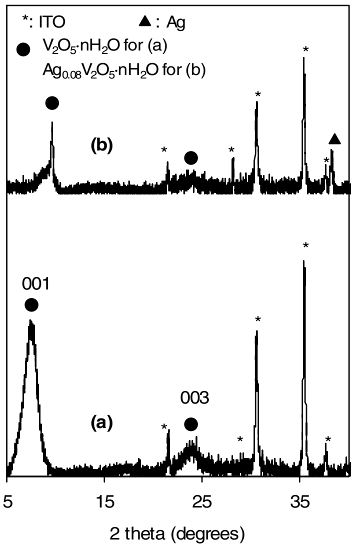

Figure 2 X-ray diffraction patterns of (a) $V_2O_5\cdot nH_2O$ film and (b) Ag–$Ag_{0.08}V_2O_5\cdot nH_2O$ film on ITO substrate.

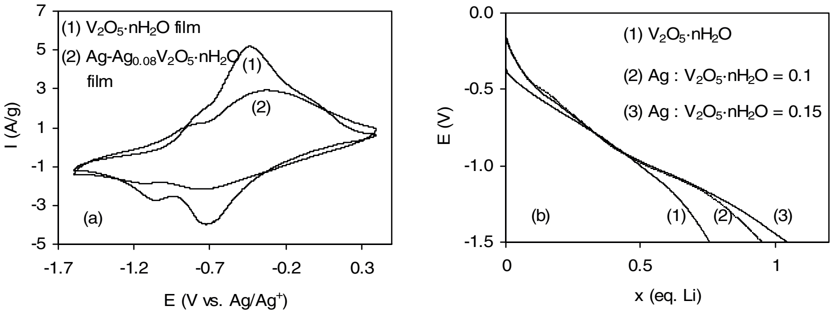

Figure 3 a) Cyclic voltammograms of Ag–$Ag_{0.08}V_2O_5\cdot nH_2O$ film and $V_2O_5\cdot nH_2O$ film in a potential range from –1.6 V to 0.4 V vs. Ag/Ag^+ and under the scan rate of 10 mV/s. b) Potential (vs. Ag/Ag^+) vs. x, i.e. equivalents of lithium intercalated, for the $V_2O_5\cdot nH_2O$ xerogel film and Ag–$Ag_xV_2O_5\cdot nH_2O$ films that have different molar ratio Ag/$V_2O_5\cdot nH_2O$. Current density 800 mA/g.

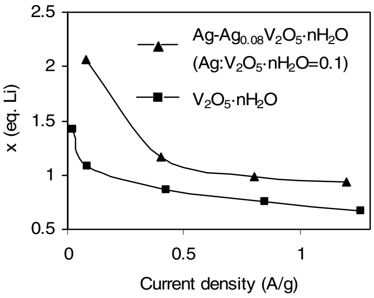

Figure 4 Relationship between current density and equivalents of lithium intercalated by $Ag–Ag_{0.08}V_2O_5\cdot nH_2O$ ($Ag/V_2O_5\cdot nH_2O$ molar ratio is 0.1) and $V_2O_5\cdot nH_2O$ xerogel film from chronopotentiometric measurements; x is equivalents of lithium intercalated for the $V_2O_5\cdot nH_2O$ xerogel film and $Ag–Ag_{0.08}V_2O_5\cdot nH_2O$ films.

V_2O_5 layers and causes the layers to be closer [9]. In conclusion, SEM images and XRD pattern of $Ag–Ag_{0.08}V_2O_5\cdot nH_2O$ indicate that the film consists of metallic Ag nanowires embedded in the matrix of $Ag_{0.08}V_2O_5\cdot nH_2O$.

Figure 3a compares the cyclic voltammograms of $Ag–Ag_{0.08}V_2O_5\cdot nH_2O$ composite film and $V_2O_5\cdot nH_2O$ film using a scan rate of 10 mV/s. The two cyclic voltammograms show broad charge/discharge peaks, characteristic of the low-crystalline nature of both $Ag–Ag_{0.08}V_2O_5\cdot nH_2O$ and $V_2O_5\cdot nH_2O$ films. However, peaks in the cyclic voltammogram of $Ag–Ag_{0.08}V_2O_5\cdot nH_2O$ film are flatter, possibly due to more amorphization in $Ag–Ag_{0.08}V_2O_5\cdot nH_2O$ film as indicated in its XRD pattern and discussed above. Although the Li^+ extraction/intercalation behaviors were found similar in the $Ag–Ag_xV_2O_5\cdot nH_2O$ composite film and $V_2O_5\cdot nH_2O$ film, the discharge capacity of $Ag–Ag_xV_2O_5\cdot nH_2O$ composite film is higher than that of $V_2O_5\cdot nH_2O$ film and increases with the amount of Ag. Figure 3b shows the chronopotentiometric curves of $V_2O_5\cdot nH_2O$ film and two $Ag–Ag_xV_2O_5\cdot nH_2O$ films that have different molar ratio $Ag/V_2O_5\cdot nH_2O$, i.e., 0.1 and 0.15 respectively.

Figure 4 summarizes the Li^+-intercalation capacity as a function of current density for $Ag–Ag_{0.08}V_2O_5\cdot nH_2O$ and $V_2O_5\cdot nH_2O$ films. We calculated the capacity based on the total mass including $V_2O_5\cdot nH_2O$ (n = 1.6 for xerogel dried under ambient condition [8]) and the entire amount of Ag, though the metallic Ag remaining in the zero-valence state (nanowires seen in SEM and indicated in XRD) is not electrochemically active. This indicates our results are conservative and the real capacity of $Ag–Ag_{0.08}V_2O_5\cdot nH_2O$ should be higher than those presented in Fig. 4. The improved electrochemical property of $Ag–Ag_xV_2O_5\cdot nH_2O$ composite film can be ascribed to changes in microstructure such as more amorphization and better electrical conduction resulting from the embedment of metallic Ag nanowires in the $Ag_{0.08}V_2O_5\cdot nH_2O$ matrix. Formation of $Ag_{0.08}V_2O_5\cdot nH_2O$ due to partial Ag reacting with $V_2O_5\cdot nH_2O$ can contribute to better electrical conduction as well, since metallic silver can be generated during the reduction cycle by the reduction of the silver ions intercalated in the material [4]. In addition, $Ag_{0.08}V_2O_5\cdot nH_2O$ exhibits both ionic conductivity arising from ion diffusion of Ag^+ and H_3O^+ and electron conductivity due to electron hopping between V^{4+} and V^{5+}. The conductivity of $Ag–Ag_{0.08}V_2O_5\cdot nH_2O$ (molar ratio $Ag/V_2O_5\cdot nH_2O$ = 0.1) film was measured by four-point probe method and was found to be about 0.1 S/cm. This conductivity is higher than the value of $V_2O_5\cdot nH_2O$ xerogel film (0.001 S/cm measured in the present study and also reported in literature [4]) by two orders magnitude, due to the Ag nanowires and formation of $Ag_xV_2O_5\cdot nH_2O$ in the composite film. In comparison with pure $Ag_{0.08}V_2O_5\cdot nH_2O$ of the same Ag/V molar ratio [4], the $Ag–Ag_{0.08}V_2O_5\cdot nH_2O$ film also shows higher electrical conductivity by one order of magnitude, due to the presence of Ag nanowires. In addition to enhanced electrical conductivity and poor crystallinity, introduction of Ag nanowires to the film and partial reaction with $V_2O_5\cdot nH_2O$ may result in introducing more porosity to the films. The apparent volume of the $Ag–Ag_{0.08}V_2O_5\cdot nH_2O$ film can be computed to be 5.0×10^{-5} cm^3 from the geometric area (0.5 cm^2) and the thickness (1 μm from cross-section SEM image (Fig. 1c). Therefore, the density of the film is calculated to be 1.4 g/cm^3, which is much lower than the reported density of $V_2O_5\cdot nH_2O$ (2.87 g/cm^3) [10]. The porosity of the composite film is estimated to be ~48%. In summary, $Ag–Ag_{0.08}V_2O_5\cdot nH_2O$ composite films have been synthesized through a simple sol–gel processing method and by dispersing pre-synthesized Ag nanowires into $V_2O_5\cdot nH_2O$ sol. The improved electrochemical performance of $Ag–Ag_{0.08}V_2O_5\cdot nH_2O$ compared to $V_2O_5\cdot nH_2O$ film is ascribed to further amorphization, increased porosity, and the enhanced electrical conductivity. Further improvement in the intercalation capacity of $Ag–Ag_xV_2O_5\cdot nH_2O$ films can be achieved with increased amount of Ag.

Acknowledgements Y.W. would like to acknowledge the financial support from the Ford Motor company fellowship. H. M. S. acknowledges the graduate fellowship from the Joint Institute of Nanoscience, University of Washington and Pacific Northwest National Laboratories. The authors would like to thank Cheng-Chun Lee for his help in using the FPP-5000 4-point probe.

References

[1] H. K. Park et al., J. Electrochem. Soc. **142**, 15 (1995).
[2] D. B. Le et al., J. Electrochem. Soc. **143**, 2099 (1996).
[3] K. Takahashi et al., J. Phys. Chem. B **109**, 48 (2005).
[4] F. Coustier et al., J. Electrochem. Soc. **146**, 1355 (1999).
[5] Y. Sun et al., Nano Lett. **3**, 955 (2003).
[6] Y. Q. Chu and Q. Z. Qin, Chem. Mater. **14**, 3152 (2002).
[7] V. Petkov et al., J. Am. Chem. Soc. **124**, 10157 (2002).
[8] Y. Wang et al., accepted by J. Phys. Chem. B (2005).
[9] S. Passerini et al., Solid State Ionics **104**, 195 (1997).
[10] Y. J. Liu et al., Chem. Mater. **7**, 1616 (1995).